



Urban Green Spaces as a Solution to Urban Heat Island: The Cooling Effect of Sétif's Amusement Park

Amor Ballout^{a,b,*}, Islam Boukhelkhal^b, Yasmina Bouchahm^b

^a Ferhat Abbas University, Sétif 1, Algeria

^b Bioclimatic Architecture & Environment Laboratory (ABE), Constantine 3 University Salah Boubnider, Algeria

ARTICLE INFO

Article history:

Received October 27, 2024

Accepted May 25, 2025

Available online May 29, 2025

Published June 26, 2025

Keywords:

Urban heat island (UHI),
Urban green spaces (UGS),
Urban cool island (UCI),
Urban Thermal comfort,
Microclimate Regulation,
Sétif Amusement Park.

ABSTRACT

The city of Sétif in northeastern Algeria has experienced rapid urbanization over the past three decades, impacting the city climate and thermal comfort conditions for residents, leading to the formation of an urban heat island (UHI) between the city center and the suburbs.

This research aims to study and evaluate the role of urban green spaces (UGS) in mitigating the UHI effect, regulating microclimates, and improving residents' thermal comfort. To investigate the role of UGS in mitigating the UHI effect, regulating microclimates and improving residents' thermal comfort, the methodology followed in this study was based on a measurement campaign conducted at Sétif Amusement Park and its surroundings during summer. While confirming Sétif's UHI, the park recorded lower temperatures and significantly improved thermal comfort compared to the surroundings. The urban park exhibited a significant cooling effect, with a maximal temperature difference of 3.3°C. Substantial improvements in thermal comfort indices were observed, including Predicted Mean Vote differences (3.30), Physiologically Equivalent Temperature (11.4°C), and Universal Thermal Climate Index (6.9°C), highlighting the park's mitigating impact on the UHI. These results demonstrate the potential of UGS to serve as cooling refreshment areas, providing relief from high temperatures and improving the overall quality of urban life.

1. INTRODUCTION

Urban areas are now home to more than 4.3 billion people, representing over half of the world's population (55% in 2017) living in cities (Ritchie & Roser, 2018). It is projected that by 2050, the number of people living in urban areas will rise by 2.5 billion, with almost 90% of this expansion

* Corresponding author, E-mail address: amor.ballout@univ-setif.dz



occurring in Asia and Africa (United Nations Department of Economic and Social Affairs Population Division, 2018).

With this rapid urbanization, there has been a substantial increase in both the population and the built environment of cities. However, this growth has led to the emergence of various environmental issues, such as the urban heat island (UHI) effect. This phenomenon is characterized by higher air temperatures in densely populated urban areas than in their suburban or rural counterparts. The primary cause of the heat island effect in cities is the absorption of solar radiation by building, roads, and other hard surfaces during the daytime. This absorbed heat is then released into the surrounding environment, increasing the ambient temperatures at night (Wong & Yu, 2005).

Urban environments have some typical characteristics, such as high population and building density, high energy consumption, and lack of green spaces. The primary consequence is the urban heat island (UHI) phenomenon, whereby air temperatures in urban environments are much higher than in rural or suburban areas (Busato et al., 2014).

Luke Howard was the first to present proof that air temperatures in cities are generally more significant than in the surrounding countryside; his evaluation of temperature records permitted him to notice, describe, and study the urban heat island phenomenon decades before others (Mills, 2008).

Since then, the Urban Heat Island (UHI) phenomenon has gained significant attention from scientists and engineers. This attention is mainly attributed to its detrimental effects on the environment and economy and the potential benefits associated with reducing high levels of thermal intensity (Memon et al., 2008).

In addition to its energy implications, elevated temperatures can intensify health risks and contribute to atmospheric pollution. Therefore, it is imperative to minimize the occurrence of Urban Heat Island during periods of high heat to promote energy conservation, public health and mitigate pollution levels (Chen & Wong, 2006).

As stated by Santamouris (2007), Akbari & Akbari (2005) and Oke (1987), identified several factors as causes of the Urban Heat Island (UHI) phenomenon. These include the low amount of evapotranspiration resulting from reduced vegetation, the absorption of solar radiation due to low albedo, the hindrance to airflow due to increased roughness, and the high amount of anthropogenic heat release. Nonetheless, additional factors also contribute to the formation of UHI, and as such, they warrant further discussion. In the following section, we will elaborate on the factors known to play a substantial role in the development of UHI, as described in Santamouris (2014).

In his paper, Nuruzzaman (2015) reviewed the causes, effects, and mitigation measures related to the urban heat island phenomenon. Among the factors that play a significant role in the creation of UHI, he cited excess waste heat and pollutants, such as greenhouse gases trapping radiation, heat emission from energy usage for heating, cooling, industry, vehicles, replacement of natural land cover with dense construction materials that retain more heat, and the lack of vegetation and trees that provide cooling through evapotranspiration and shading.

The planting of vegetation in urban areas is a key strategy for mitigating the effects of the UHI, because vegetation plays a vital role that vegetation plays in regulating the urban climate. This is an effective measure for creating an 'oasis effect' and reducing urban warming at both macro and micro levels (Chen & Wong, 2006).

Even a single tree can help to create a more comfortable microclimate. However, arranging vegetation in large areas such as urban parks, neighborhood parks, rooftop gardens, and other areas can have a significant effect on the energy balance of the entire city. This is because of the increase in evaporation

surfaces as well as the amount of surface areas that are shaded by the tree canopy (Alonzo et al., 2021; Jauregui, 1990).

The impact of vegetation on climate change has direct and indirect consequences. The indirect influence results from the emission and sequestration of greenhouse gases, which are influenced by climate change. The direct effect, on the other hand, pertains to the influence of plants on the distribution of incoming solar energy, including processes such as reflection, evapotranspiration, sensible heat, ground heat flux, and photosynthesis. These processes have a crucial role in regulating the daily temperature (Huryňa & Pokorný, 2016).

Urban vegetation consists of various forms like street trees, public parks and gardens, private gardens, green roofs, vertical gardens, urban farms and community gardens, median strips and traffic islands, that contribute to the environmental, social, and aesthetic aspects of urban environments. In this study we will focus on the effect of urban parks. Urban parks represent concentrated areas of vegetation and greenspace that provide significant ecosystem services to cities. Compared to other scattered forms of urban greenery like street trees or private gardens, urban parks create larger uninterrupted zones of cooling through shading and evapotranspiration (APPA, 2019; Edwards et al., 2020; Carne, 1994; Sukopp & Werner, 1983).

Beyond their aesthetic value, urban parks impact positively human health and wellbeing through recreational and leisure activities, contribute to social cohesion and identity by strengthening social ties, attract tourism and increase the value of real estate. Additionally, urban parks promote biodiversity, species diversity, ecosystem functioning and a range of ecosystem services, reduce air pollutant levels, contribute to carbon sequestration, regulate stormwater and run-off, and play a role in cooling urban areas. Overall, urban parks are essential assets to urban environments, and their benefits positively impact both humans and the surrounding ecosystem (Carne, 1994; Konijnendijk et al., 2013).

Urban parks are consistently linked to the urban cool island phenomenon (UCI), which is characterized by the noteworthy observation that parks, green spaces, and vegetation in urban areas tend to be noticeably cooler than the surrounding built-up neighborhoods and city structures (Yang et al., 2016).

Urban parks can mitigate the urban heat island (UHI) phenomenon, effectively improve the urban microclimate, and enhance thermal comfort. Numerous empirical studies have shown that urban parks can cool and humidify the surrounding environment through evapotranspiration, shading, and water, playing a leading role in reducing urban land surface temperature, and dissipating absorbed radiation in the form of latent heat (Zhang et al., 2023).

The present study aims to quantify the effects of the leisure park of the city of Sétif on the comfort conditions of pedestrians and users during the hot season compared to highly dense urban areas, with a specific focus on assessing different climatic parameters such as air temperature and relative humidity, as well as three well-used comfort indices (PMV, PET, and UTCI) that provide a comprehensive understanding of pedestrian thermal comfort in the two environments. By analyzing these parameters and indices, this study sheds light on the relationship between urban parks and environmental conditions, offering practical advice for urban planning and design to improve thermal comfort in cities.

2. DATA AND METHODS

Studies on the impact of vegetation and urban parks are usually categorized into three groups based on the type of data utilized in the research. The first category comprises research that use meteorological data and satellite imagery to examine the effects of green spaces on a large scale, offering a

comprehensive view of how vegetation affects urban areas on a large level (Choi et al., 2012; Corocăescu et al., 2023; Huerta et al., 2021; Sunita et al., 2021).

The second category involves more detailed assessments through in-depth field measurements at the micro level to provide a thorough understanding of the specific effects of greenery in urban environments. These investigations frequently require actual observations and measurements to catch more details that may not be overlooked when employing extensive data sources (Algretawee, 2022; Ballout et al., 2016; Kulish, 2022; Matallah et al., 2020; Mikami et al., 2015; Sugawara et al., 2016; Xiao et al., 2018; Yan & Dong, 2015).

The third category uses numerical simulations and computations to predict the thermal benefits provided by green spaces in urban areas. Researchers can use modelling techniques and computational tools to forecast and measure the cooling effects and other thermal advantages of urban vegetation. This information can offer valuable guidance for urban planners and policymakers seeking to improve the sustainability and quality of urban areas (Alves et al., 2022; Ballout et al., 2015; Boukhelkhal & Bourbia, 2016; Qin et al., 2021; Simon et al., 2021; Stark da Silva et al., 2023; Yang et al., 2021).

The various methods used in these categories help provide a thorough comprehension of how vegetation impacts urban microclimates and highlights the multiple advantages that green spaces provide in reducing the Urban Heat Island effect and environmental issues in densely populated regions.

In this study, we used the second method for several reasons. First, field measurements provide empirical data that can be used to quantify the impact of UGS on various environmental and human health parameters such as air temperature, relative humidity, wind speed, T_{mrt} , and thermal comfort indices like PET, PMV and UTCI. These empirical evidences are essential to establish a scientific basis for understanding the specific benefits of urban vegetation in the study area. Second, field measurements allow for the assessment of the spatial and temporal variability of the effects of vegetation, which will allow us to have a microclimatic scale view that will help us to conduct a timescale study of the comfort in the study area and this for a full day. Finally, such measurements provide a foundation for the validation of models and simulations that can be used in further studies, ensuring that predictions and projections related to the effects of vegetation are accurate and reliable. Therefore, in-depth field measurements play a critical role in advancing our understanding of the various effects of urban vegetation and plant cover existing in the park on user comfort and the creation of an urban cool island (UCI) in this area.

In addition, we employed bivariate correlation plots to examine, comprehend and quantify the relationships between the different thermal comfort indices (PET, PMV and UTCI) and the environmental parameters (T_a , H_r , V_a and T_{mrt}) and thereby underscore the importance of vegetation that affect each of these parameters.

We would like to point out that we opted for a monofactorial approach focusing specifically on the impact of vegetation while acknowledging the presence of other variables (materials, inertia, human activities, urban pollution and urban geometry) that contribute to thermal variations. This methodological choice offers distinct advantages, including the ability to isolate and quantify the influence of a specific variable with greater clarity, simplify experimental design, and draw more direct causal relationships.

The true originality of our study lies in its rare contextual application. While the methods themselves are well-established, the application of these methods to a large urban park in a geographical setting that has been rarely studied represents a significant contribution. Specifically, our research focuses on Sétif Park in Algeria, a region where scientific literature on the microclimatic effects of urban parks remains extremely limited. In fact, studies on urban parks in Africa, and particularly in Algeria, are scarce, with

the city of Sétif being entirely unexplored in this regard. Most existing studies in the region have focused on small green spaces or isolated vegetation configurations, leaving a critical gap in understanding the thermal dynamics of large urban parks in semi-arid climates.

2.1 Study area

The city of Sétif is located in the north east of Algeria at (36° 09' 00"E, 5° 26' 00"N); it is one of the most populated cities in this country. It has a continental Mediterranean semi-arid climate (Csa) according to the Köppen-Geiger climate classification, with hot and dry summers and cold and rainy winters.

According to the climatic data recorded between 1991 and 2021, it is evident that the average air temperature reaches its highest level in July (24.4°C) and its lowest level in January (4.4°C). Similarly, the maximum air temperature is observed in July (31.4°C), whereas the minimum air temperature is recorded in January (0.5°C). Moreover, the average yearly relative humidity ranges between 43% and 77% (Climat-data, 2023).

The on-site experiment was conducted in an urban park in the city of Sétif, named the municipality Amusement Park. This park (30 hectares) is located in the city center, contains an important amount of vegetation (especially in the northern part of the park) and located near two main districts with different characteristics and typologies (Fig. 1). The first is the old city downtown, situated south of the park, with a high-density build environment, a large commercial activity on the ground floor of construction and a dense and a high traffic along this street. The second one situated north of the park is the district of 600 dwellings, a relatively new settlement (70's) with a low build density, both areas present a high level of minerality and a very low density of vegetation (Fig. 2). Practically no commercial activity found in this area but a high a dense and a high traffic along this street, but a large concentration of tertiary and residential activity with large parking area all throughout this space.

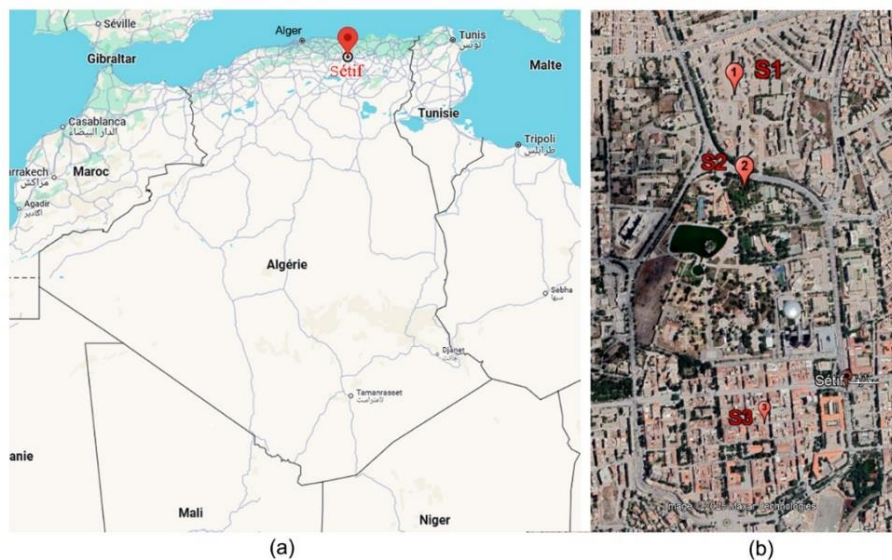


Fig 1. (a) Sétif city location: (b) The three stations in the investigation site.

The selection of measurement points used a dual approach, combining site typology assessment with user feedback obtained through questionnaires. This methodology integrated both physical characteristics of the sites and user experience data to ensure comprehensive sampling coverage. The site typology analysis considered vegetation density, spatial configuration and urban context, while the questionnaire responses provided insights into user patterns and thermal comfort perceptions. This

combined approach enabled us to strategically position measurement points that would capture both the physical variability of the environment and areas of significant user interaction.

For more details concerning the spatial configuration, the three points were chosen in the three different spaces with different landscape types and typologies:

The first (S1) was placed within the 600 dwellings district in a semi-open space with height/width ratio $H/W=0.4$ (Fig.3.B), characteristic of sparsely populated urban areas or residential neighborhoods with wide streets in relation to the height of buildings. And an $SVF=0.493$ (Fig.2) equivalent to a moderate level of obstruction that still allows significant access to solar radiation and thermal exchanges with the atmosphere.



Fig 2. Study sites configurations.

Figure 2 highlights the typological differences between the three measurement sites. The urban park, unlike the two urbanized areas, has almost no built structures, making it a rare natural space within the city. This distinction is crucial, as our study aims to contrast the thermal behavior of densely built environments with that of a vegetated area.

Buildings around this space are typical of architectural style of this period and construction methods. These structures are characterized by multi-story residential blocks with concrete frame construction, standardized design, prefabricated elements, repetitive window patterns, and simple geometric forms. The main construction materials include reinforced concrete structure, standard brick panel for the facades, single-glazed windows, basic insulation materials, and flat roof construction (Fig. 2). Regarding their thermal properties, these buildings feature low thermal mass construction with poor thermal insulation by modern standards. The ground around the measurement point was constituted of asphalt (roads, parking and sidewalks), characterized by high thermal inertia.

The second point (S2) was placed within the park under the densest tree canopy in this area, $SVF=0.05$ meaning that the measuring point is located under an extremely dense vegetation cover where only 5% of the sky is visible through the foliage (Fig.2). No remarkable buildings or constructions are located around the measurement point and the floor was consisting mainly of grass or bare soil.

The third (S3) was placed in a narrow street within the city downtown without any vegetation, and with a H/W ratio of 1.55 indicating a fairly deep urban canyon (Fig.3.A), typical configuration of historic city centers and an $SVF=0.25$ (25% of the sky is visible from the observation point) (Fig.2). This is a typical value found in dense urban configurations. The implications of this ratio are the limited access to direct sunlight.

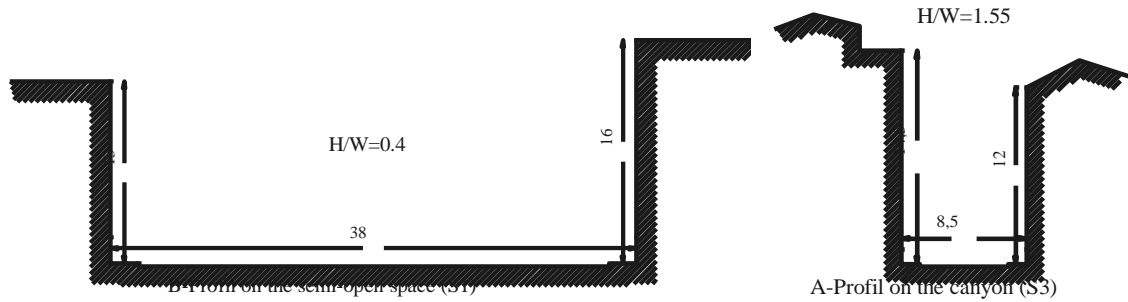


Fig 3. Profile of the Semi-open space and the canyon.

The buildings on both sides of the canyon are French colonial buildings constructed in Sétif between 1840-1860 represent a distinctive architectural style, characterized by thick limestone and stone masonry walls (40-60 cm), combined with high ceilings (3.5-4 meters) and inner courtyards and small deep-set windows. The ground around the measurement point was constituted of asphalt (road) and standard pavement (sidewalks), characterized by high thermal inertia as stated for S1. All three measurement points were located at similar elevations, with S1 at 1092 m above sea level, S2 at 1090 m, and S3 at 1087 m.

2.2 Field measurements

In situ measurements were performed in summer on August 2, 2017, which was part of the hottest period in the city of Sétif. Meteorological parameters, including air temperature (T_a), relative humidity (RH), wind velocity (V_a), mean radiant temperature (T_{mrt}), Predicted Mean Vote (PMV), and Predicted Percentage of Dissatisfied (PPD), were measured using the HD32.2 WBGT Index instrument (Delta OHM, Italy) (Fig. 4).



Fig 4. HD32.2 WBGT Index instrument (Delta OHM, Italy)

All measurements were made 1.2m above the ground, and the data were recorded every 60 min for 24 hours (from 01:00h to 00:00h). All measurements were performed on a sunny day without strong winds or cloudy conditions. To prevent interference from solar radiation and obtain accurate measurements, three points were placed in shaded areas.

Climatic data, including air temperature (T_a), relative humidity (RH), and wind velocity (V_a), were also collected from the Esfiha Meteorological Station (ID: AGE00147713) located in the suburban region of the city, and were compared with the measurements collected in the study area. A fisheye lens (Sigma 8 mm circular) was used with a Nikon D700 digital camera to assess the sky view and capture fisheye photographs of the three spaces (Fig.2).

2.3 Thermal comfort indices

Air temperature, relative humidity, and wind speed are indeed important factors that should be considered when studying thermal comfort. However, these factors alone may not provide a comprehensive assessment of thermal comfort (Dec et al., 2018; Li et al., 2017; McIntyre, 1973).

Therefore, comfort indices such as PMV, UTCI, and PET have been developed to address these limitations by incorporating additional environmental factors and the physiological responses of occupants. While air temperature, relative humidity, and wind speed are essential components of the thermal environment, they do not account for factors like personal factors, solar radiation, shading and ventilation, and thermal adaptation (Walls et al., 2015).

For these reasons, we used the three comfort indices in order to have a substantially advanced understanding of the complexity of human thermal comfort responses. The three indices are:

2.3.1 Predicted Mean Vote (PMV)

The predicted mean vote (PMV) is a commonly used index for evaluating thermal comfort in both indoor and outdoor environments. It is based on the heat balance of the human body and is used to predict the average vote of a large group of people regarding the thermal sensation of a given environment. The PMV scale ranges from -3 to +3, where -3 indicates cold discomfort and +3 indicates hot discomfort. This index considers factors such as air temperature, radiant temperature, air speed, and clothing insulation to provide a quantitative measure of thermal comfort (Laouadi, 2022; van Hoof et al., 2017; Nicol & Humphreys, 2002).

While PMV is a widely used index for assessing thermal comfort, it has some limitations that need to be considered when evaluating thermal comfort in different environments, and some studies have suggested that PMV may not be suitable for outdoor environments because applying the PMV equation to outdoor conditions in summer heat stress situations can easily produce PMV values higher than +4 (+8 and more). While this result violates the range of the original PMV system it is numerically correct (Gatto et al., 2020; ENVI-met, 2023).

Other thermal comfort indices, such as the Universal Thermal Climate Index (UTCI) and Physiologically Equivalent Temperature (PET), have been developed to address some limitations of PMV in outdoor environments (Laouadi, 2022; Fang et al., 2017; Lenzuni, 2021; Nicol, 2004; Wu et al., 2022; Salameh et al., 2023).

Despite this, we believe that the use of PMV for academic research is quite acceptable even if the values are higher than +4, and can be considered adequate for comparison, even more if these values were directly measured with the HD32.2 WBGT Index instrument (Delta OHM) and not calculated. A comparison of the PMV values measured at the three sites is still very useful in the assessment of thermal comfort in the study area.

2.3.2 Physiologically equivalent temperature (PET)

Based on the human energy balance and calculated by a mathematical model, it is among the most used indices in the analysis of thermal comfort in outdoor environments, as it accounts for the influences of air temperature, humidity, wind speed, and sun radiation on the human body (Höppe, 1999).

The physiological equivalent temperature (PET) is ideally suited for the assessment of the thermal component of a wider range of climatic regions than the other indices. Compared to other thermal indices like (PMV), PET is more advantageous due to its use of degrees Celsius (°C) as a unit of measurement. This makes the results easier to understand for urban and regional planners who may not be well-versed in contemporary human biometeorological terminology (Matzarakis et al., 2014).

The Physiologically Equivalent Temperature (PET) has been used widely, mainly in urban planning and architectural research. Its popularity comes from its relative simplicity and its long history in studies related to UHI, microclimate analysis, and outdoor comfort. Although less detailed than UTCI, PET remains a preferred tool because of its ease of application in urban contexts (Liu et al., 2023).

The use of such software tools is common practice in the assessment of outdoor thermal comfort because of their ability to efficiently compute the PET index. These software are commonly used in the assessment of outdoor thermal comfort because of their ability to efficiently compute the PET index (Chen, 2023; Paris et al., 2022; Pezzoli et al., 2012).

The Physiologically Equivalent Temperature (PET) can be easily computed using different software applications. In this investigation, we used the Ryman Pro program to calculate the PET values.

2.3.3 The Universal Thermal Climate Index (UTCI)

The UTCI is a bioclimatic index which represents physiological comfort of the human body under specific meteorological conditions (Bröde, 2021). In addition to the ambient temperature, additional factors including humidity, wind speed, and mean radiant temperature are considered, to have a substantial impact on the physiological response to the surrounding environment (Błazejczyk et al., 2013).

The UTCI is intended to be applicable at all spatial, temporal, and climatic scales. Based on human heat balance models, it is widely used to evaluate thermal comfort in outdoor and semi-outdoor urban areas (Bröde et al., 2012).

The Universal Thermal Climate Index (UTCI) is widely known as a more comprehensive tool for evaluating thermal stress. Its complexity allows it to consider a wider range of environmental conditions, making it highly suitable for various climates and applications, from urban environments to global climate studies. This is mainly because the UTCI takes into account not only air temperature but also factors such as wind speed, humidity, and radiation, which improves its precision in different settings, including extreme climates conditions (Liu et al., 2023).

The UTCI's intricate nature enables it to account for a broader spectrum of environmental factors, making it exceptionally adaptable for diverse climates and uses, ranging from city landscapes to worldwide climate research. This versatility stems primarily from the UTCI's consideration of multiple variables beyond air temperature, such as wind velocity, moisture levels, and solar radiation. By incorporating these additional factors, the UTCI achieves greater accuracy across various settings, including harsh climate conditions.

We determined the UTCI values by using the Rayman Pro software, one of the most used instruments for comprehending and enhancing thermal comfort in urban environments.

In order to validate the outcomes derived from the Rayman Pro software, we verified the results using the Climate CHIP's Heat Stress Index calculator, a tool provided by the Climate CHIP organization (Climate Change Heat Impact & Prevention | Climate CHIP, 2024), aimed at estimating heat stress levels experienced by individuals in various environmental conditions and calculating several indices such as Wet-Bulb Globe Temperature (WBGT) and Universal Thermal Climate Index (UTCI). The above-mentioned validation procedure served to substantiate the reliability of the outcomes produced by Rayman Pro and reinforced our convictions concerning the thermal advantages associated with urban vegetation on the outdoor thermal comfort.

3. RESULTS AND DISCUSSION

In this study, we aimed to investigate the role of urban parks in ameliorating thermal comfort in Sétif, Algeria, by analyzing various parameters such as air temperature, relative humidity, wind speed, Tmrt, PMV, PET, and UTCI. The results presented in the following sections demonstrate the impact of urban parks on thermal comfort and provide insights into the factors that influence comfort in outdoor spaces.

As we proceed with the analysis, we first present the results related to air temperature, relative humidity, wind speed, and Tmrt, followed by the analysis of PMV, PET, and UTCI values. By examining these parameters, we gain a better understanding of the role of urban parks in providing thermal comfort and mitigating the urban heat island effect.

3.1 Air Temperature Variations

Figure (5) shows the air temperature variation for different land cover types during the day of investigation. It is noticeable that the air temperature at all three points reached the minimum value at 06h00, and the lowest temperature values were in the order of: Downtown (26.3°C) > 600 dwellings (25.6°C) > Park (24.0°C). The temperature rises in the middle of the day, reaching the maximum for the three points at 14h00, having values of 41.9°C for the 600 dwellings (S1), 41.5°C for the downtown (S3), and 40.0°C for the park (S2). In the late afternoon, the temperature decreases in the three stations until it reaches 30.2 °C for (S1), 29.8 °C for (S3), and 27.7°C in the park (S2).

The measurements show that the park is clearly cooler than the surrounding areas throughout the day. Temperature differences among land cover types were practically stable throughout the day, presenting a mean difference of 2.1 °C between S2(park) and S1(600dwl), reaching 3.3 °C at 11h00 as a maximum value and a mean value of 1.8 °C between S2(park) and S3(downtown) reaching 2.6 °C at 19h00 as a maximum value (except certain periods).

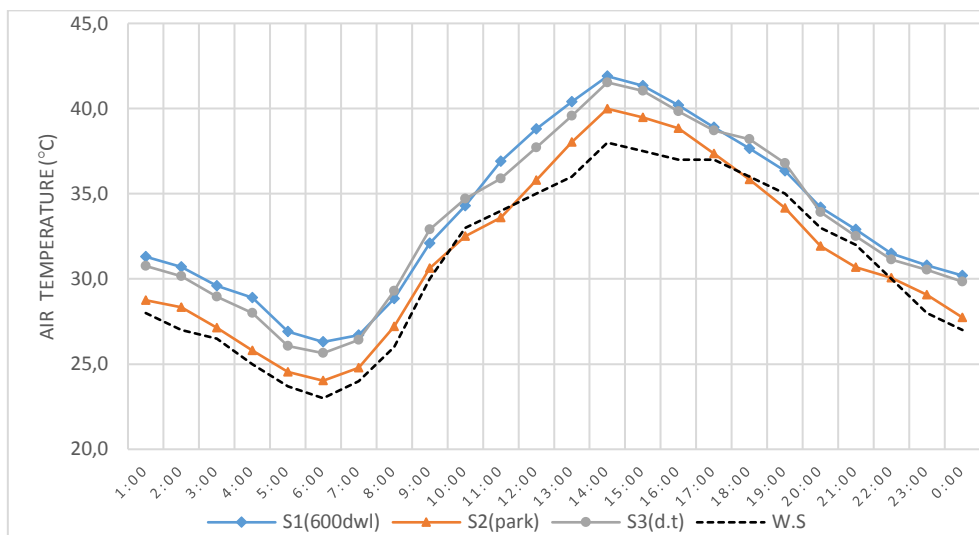


Fig 5. Air temperature for three sites of investigation and weather station.

When point S2 benefits from the park (especially from vegetation) both points S1 and S3 are situated in locations with a combination of asphalt pavement and massive walls significantly (for S3) and concrete (for S1) influences outdoor thermal stress. The asphalt surface, characterized by its high solar absorption coefficient (0.85-0.95) and low thermal reflectivity, acts as a heat sink during the day. This stored heat is then released during the evening and night hours, contributing to the deterioration of outdoor thermal comfort. Additionally, the building's massive walls, while providing indoor thermal comfort through their high thermal inertia, also participate in the outdoor heat stress by storing solar radiation during the day and releasing it gradually. This creates a combined effect where both horizontal (ground) and vertical (facades) surfaces contribute to increased air temperatures and mean radiant temperature in the urban space, particularly affecting pedestrian comfort during heat stress periods. This thermal behavior is especially pronounced in urban canyons where the interaction between asphalt and building facades can create localized hot spots with reduced thermal comfort.

By comparing (S1) and (S3), the measures show that the 600 dwellings (S1) were warmer than the downtown area (S3), with an average of 0.5 °C and a maximum value of 1.1 °C at 12h00, except for the periods 8h00-10h00 and 18h00-19h00 where the downtown area became warmer than the 600 dwellings area.

This is comparable to the work presented by (Chen & Wong, 2006), who conducted on-site measurements of microclimates in two urban parks in Guangzhou, China, and compared them to the surrounding built-up areas. Data on the air temperature, relative humidity, and wind speed were gathered from multiple locations throughout the morning and afternoon periods, and a significant cooling effect was observed within the park. The average temperature contrast between the park's interior and its environs was 2.18°C, with the park being as much as 3.5°C cooler during daylight.

The temperature reduction caused by Sétif urban park found in our study corroborates the findings of Bowler et al. (2010), Chang & Li (2014), Park et al. (2021) and Qiu et al. (2023) whom also identified significant cooling effects of green spaces ranging between 2-5°C in various cities.

In comparison with the weather station (W.S), we noticed that the three stations were warmer than the weather station for almost the entire investigation day. The mean value of the difference between the weather station and (S1) (600 dwellings) was 2.7°C and the maximum value was 4.4°C; for (S3) (downtown), the mean difference was 2.4°C and the maximum value was 3.6°C and for (S2) (park), the mean difference was 1°C and the maximum value was 2°C. These results confirm the presence of UHI in the city of Sétif. The only exception was the park station (S2), which was cooler than the (W.S.) at 10h00 and in the interval 18h00-21h00.

3.2 Relative Humidity Variations

Figure (6) shows the relative humidity (Hr) variation in the three points during the day of investigation. It reaches the maximum value at 06h00, having an inverse order compared to the air temperature, the order of relative humidity values was:

Park (56.0%) > 600 dwellings (48.5%) > downtown (45.3%); this order was respected throughout the day. In the middle of the day, the relative humidity reached a minimum value for the three points at 13h00 (instead of 14h00 for the maximum temperatures). The values were 13.9% for 600 dwellings (S1), 14.3% for the downtown area (S3), and 17.9% for the park (S2). At the end of the day, the humidity increased until it reached 38.4 % for (S1), 41.2 % for (S3), and 47.6% in the park (S2).

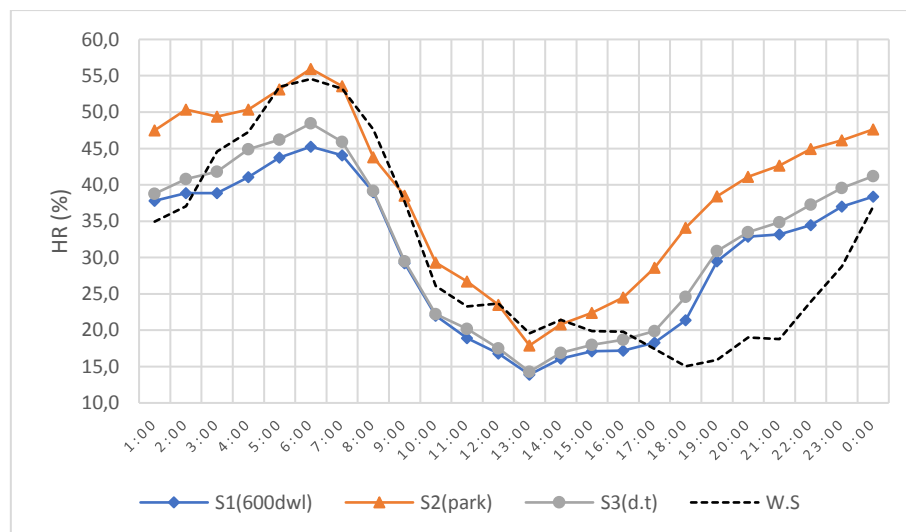


Fig 6. Relative humidity for three sites of investigation and weather station.

The park (S2) is wetter than the other sites (S1 and S3) during the day, where relative humidity differences fluctuate between 4.0% and 12% between the park (S2) and the 600 dwellings (S1), 3.6% and 9.5% between the park (S2) and the downtown (S3), this makes a mean difference of 8.6% between S2 (park) and S1(600dwl) reaching 12.7% at 18h00 as a maximal value, and 6.9 % between S2(park) and S3 (downtown) and 9.5% at 19h00 as the maximal value.

The work of Chen & Wong (2006) also confirmed such values with the average of relative humidity recorded inside urban parks, which was approximately 13% higher than that of the surrounding neighborhoods. In our case, this can be explained by the effect of the dense canopy of the trees, not only reducing wind speed but also increasing humidity in the air and reducing water loss from the soil.

The measurements show that the downtown (S3) is more humid than the 600 dwellings (S1), with an average of 1.7% and a maximum value of 3.8 % at 4h00, this difference is more pronounced at the beginning and the end of the day and decreased in the middle of the day.

Except for S1, stations S2 and S3 are globally more humid than the suburbs (W.S), which was achieved by comparing the mean relative humidity throughout the day of investigation (S1=30.2%, S3=31.9%, S2=38.8%, and W.S=30.8). We noticed that the park is clearly wetter than all its surroundings and is also wetter than the suburbs, which is due to the effect of evapotranspiration of the trees and grass that covers the area of station S2.

The curve of relative humidity of the W.S has a similar shape to the three urban locations studied, except for the period between 16h-00h00 where the values decrease abnormally. This behavior of the humidity curve is due to the increase of wind speed during this period (Fig. 6.), which sweeps away water particles from the air and soil, lowering humidity (Ravi & D’Odorico, 2005; Zakaria et al., 2020) at the end of the day.

3.3 Wind speed Variations

Based on the wind speed data, the results indicate that the park (S2) had lower mean and maximum wind speeds than the other stations (S1 and S3). Similarly, the minimum wind speeds at S2 were lower than those at S1 and S3 (Fig.7). These findings suggest that trees have a significant impact on wind speed because areas under the canopy tend to have lower wind speeds than open areas without trees. Studies have shown that the presence of trees can lower wind speeds by an average of 0.2 m/s (Huang et al., 2020) and can significantly reduce wind speeds by up to 1.0 m/s under high percentage canopy cover (Sanusi et al., 2016).

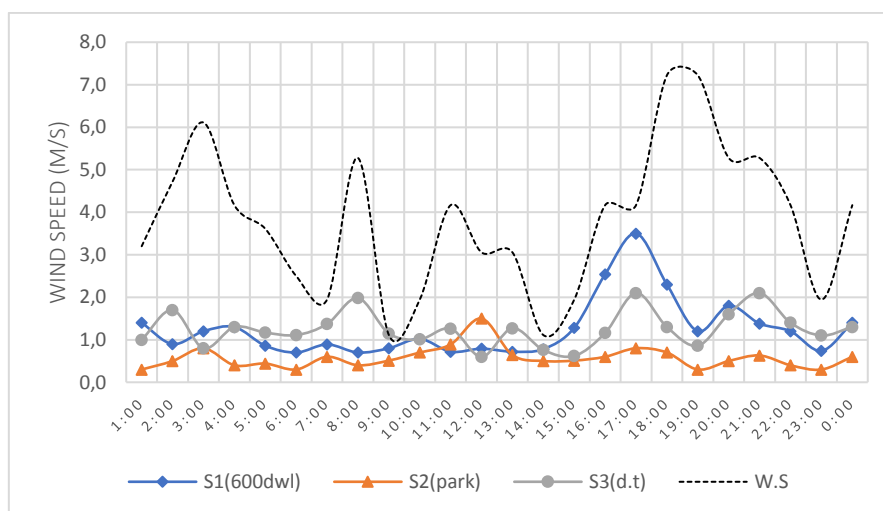


Fig 7. Wind speed for three sites of investigation and weather station.

Due to the presence of windbreak and wind sheltering effect, we can say that the presence of tree canopies significantly reduced wind speed in comparison to areas with no such barriers, such as S1 located in an open area or S3 situated within a canyon that accelerates wind speed due to its geometry.

In addition to natural and artificial barriers (buildings), other local factors such as surface temperature variations, urban geometry, and terrain roughness and topography can influence wind speeds in specific urban areas. Our observations also revealed that wind speeds were higher in suburban areas than at the three urban locations (W.S mean = 4.1 m/s, W.S max = 9.2 m/s, W.S min = 1.1 m/s), which can be also attributed to the differences in roughness between the two sites and the absence of obstacles near the weather station. Many studies showed that urban geometry has a significant influence on wind flow and natural outdoor ventilation, with direct impacts on thermal comfort (Bouketta & Bouchahm, 2023; Du & Mak, 2018).

As previously mentioned, the increase in wind speed during the later hours of the day had an impact on the relative humidity levels near the weather station, resulting in a noticeable drop in the latter (Fig. 6.).

3.4 Mean Radiant Temperature (Tmrt) variations

The mean radiant temperature (Tmrt) curve for station S2 (park) was significantly lower than those for stations S1 and S3. This is mainly because of the solar masks generated by the canopy of trees, which decrease or completely eliminate direct solar radiation gains. Additionally, these shading effects decreased the temperature of various surfaces surrounding station S2.

The shape of the Tmrt curves for the three stations is directly related to the solar masks of the different obstacles (Fig. 8), whether they are natural as trees (in the case of station S2) or artificial as buildings (in the case of station S1), which is located in a semi-open space, or S3, which is located in an urban canyon.

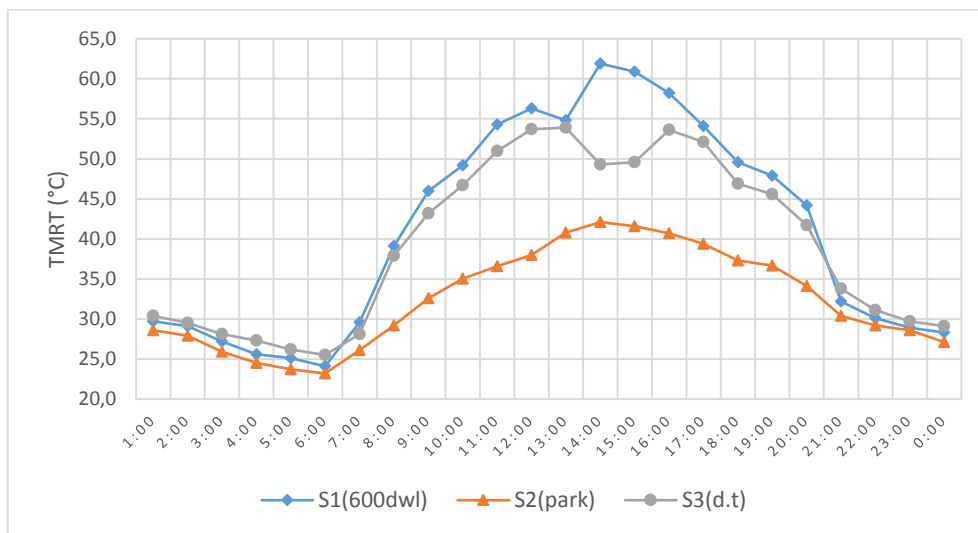


Fig 8. Mean radiant temperature for three sites of investigation.

Station S2 benefited the most from the effect of solar masks and recorded the lowest Tmrt values compared with S1 and S3. The average day value is 32.1 °C for S2, 41.7 °C for S1, and 42.6 °C for S3, which is a decrease of 10.5 °C (between S2 and S3). The same logic was noticed for maximum values with 43.5 °C for S2, 59.1 °C for S1, and 69.5 °C for S3. For the minimum values, S2 is the coolest station with 20.9 °C, but the only difference is recorded between S1 and S3, where S3 is cooler with 24.1 °C compared to S1 with 25.4 °C. It should also be noted that the difference in Tmrt can reach up to 27.9 °C between S3 and S2 at 4 p.m. and 16.8 °C between S1 and S2. Sanusi et al. found similar

results with 12°C in their study (Sanusi et al., 2016). Thom et al. (2016) found that increasing tree cover can significantly reduce Tmrt, with the greatest reductions (14.1 °C - 18.7 °C) observed in areas with high tree density. Hanafi & Alkama (2016) also found 14.9 °C of difference in their study.

The comparison between S1 and S3 reveals that the S3 station records lower Tmrt values than those recorded in S1 for more than 15 hours of the day (mostly at the beginning and end of the day), with an average of 1.9 °C, a maximum of 2.9°C, and a minimum of 1.0°C. For the rest of the day, station S1 recorded values higher than S3, but the variations were more significant, with an average of 6.6 °C, a maximum of 11.4 °C, and a minimum of 3.0 °C.

This difference in the behavior of the Tmrt curves of these two stations is mainly due to the difference in the geometry of the spaces in which the two stations are located, where S1 is in a semi-open space and S3 is in an urban canyon oriented east-west, which offers a solar mask in the middle of the day to this station; hence, the abnormal decrease in the values of this curve between 13:00 and 16:00.

The fact that the recorded Tmrt values in S3 were significantly higher than those recorded in S1 during midday can be explained by the heat gains from the north canyon walls (facing south) due to direct solar radiation on those walls during this period. This is in contrast to S1, which is located in a semi-open space and faces no walls on for directions.

3.5 Physiologically Equivalent Temperature (PET) variations

First, we noted that Tmrt significantly influenced the shape of the Physiologically Equivalent Temperature (PET) curves for the three stations. Additionally, the overall shape of the two temperatures (Tmrt and PET) seems to have a strong relationship, unlike various climatic parameters, such as air temperature, relative humidity, and especially wind speed. Several studies confirmed this observation, such as (Mayer et al., 2009). This study used the PET to quantify the level of human thermal comfort and found that the total radiation heat accumulated in the mean radiant temperature Tmrt mainly determined the PET conditions at both studied sites.

Generally, the PET curve for station S2 was below the curves for stations S1 and S2 (Fig. 9) because of the beneficial effects of the vegetation cover of the park. In addition, station S3 seems more comfortable than station S1, because station S3 was located in the middle of an urban canyon (Fig. 3), taking advantage of the solar shading of the buildings around this point, unlike the open space where station S1 was located.

Station S2 (park) was far more comfortable than stations S1 and S3 because of the beneficial effects of trees. It records an average PET value of 31.7°C, while S3 (downtown) records 35.4°C and S1 (600 dwellings) 36.8°C, this is equivalent to an average difference of 3.7°C and 5.1°C respectively. Maximum values also followed the same pattern, with 41.8 °C for S2 at 13:00, 47.2 °C for S3 at 16:00 and 53.2 °C for S1 at 14:00. The maximum difference between S2 and S3 was 9.1°C at 12:00 and 11.4°C between S2 and S1. Mayer and al. found in their studies that the peak difference was 12.5 °C around 14h00 (Mayer et al., 2009). The difference can even exceed 20°C, as it was found by Holst (Holst & Shashua-Bar, 2010).

A comparison of the two stations S1 and S3, reveals that S1 was 1.4°C warmer than S3 on average. The maximum difference between the two stations was 6.5°C at 14:00, with S3 being more comfortable due to the canyon geometry, which created significant solar masks (Abd Elraouf et al., 2022).

It is noticed that the PET curve for station S3 exceeded that for station S1 (from 00:00 to 03:30 and from 21:00 to 24:00), due to the trapping effect of the buildings on either side of the street, which reduces the percentage of visible sky and therefore reduces radiative exchanges between the canyon and the sky,

unlike station S1, which is located in an open space that promotes night-time exchanges with the sky, which is more visible.

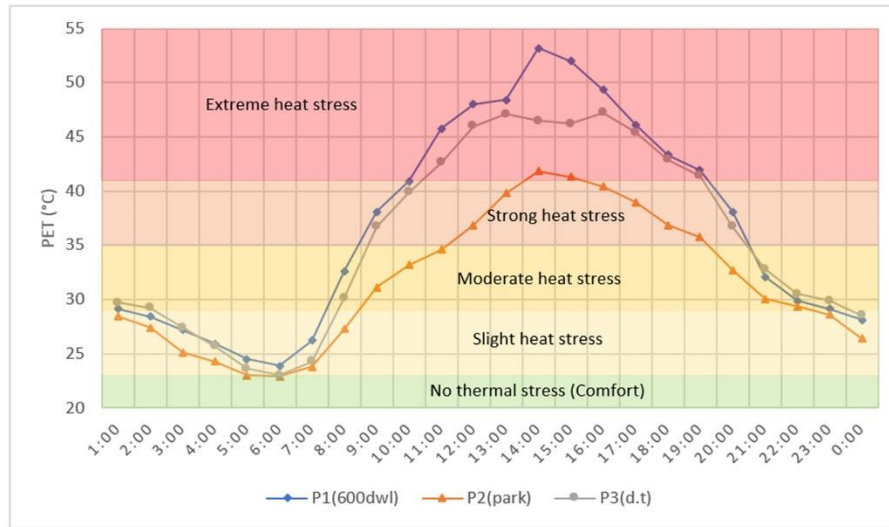


Fig 9. Physiologically Equivalent Temperature (PET) for three sites of investigation.

Station S2 was considerably more comfortable, as the PET curve was mainly located in more comfortable areas than the curves of stations S1 and S3. This was clearly noticeable during the extreme heat stress period (recorded mainly in the middle of the day). The curve lies practically outside this zone of extreme stress, with a duration of just 1 h 45 (7.5% of total daily time), in contrast to S3 with almost 8h30 hours of extreme stress (35.5% of total time) and S1 with 9 h 15, representing 38.5% of total daily time.

We notice that all three stations do not reach the comfort zone during the whole day, except station S2 which touches this zone for an hour approximately at the beginning of the day (between 5:00 and 6:00) representing 4% of the whole day, whereas S1 and S3 does not even reach this comfort zone throughout the day. This reflects the extreme heat stress during the day of investigation.

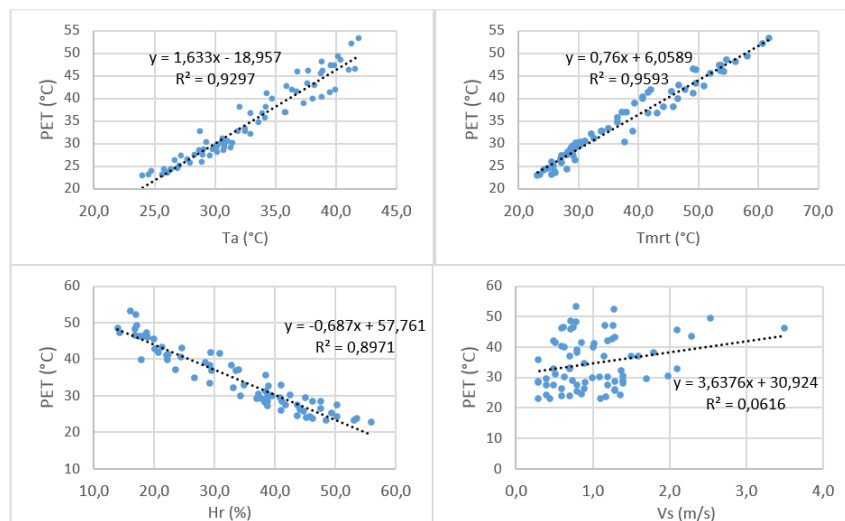


Fig 10. Correlation between (PET) and various environmental parameters.

Figure (10) presents four scatter plots showing the relationship between Physiological Equivalent Temperature (PET) and various environmental factors, with corresponding linear regression equations and R^2 values indicating the strength of these relationships. In the top-left plot, PET is positively

correlated with ambient temperature (T_a), following the equation $y=1.633x-18.957$, with a strong positive correlation ($R^2 = 0.9297$). The top-right plot shows a similar positive correlation between PET and mean radiant temperature (T_{mrt}), represented by $y=0.76x+6.0589$ and ($R^2 = 0.9593$), suggesting an excellent fit. In contrast, the bottom-left plot reveals a negative correlation between PET and humidity (H_r), with the equation $y=-0.687x+57.761$ and ($R^2 = 0.8971$), indicating a strong inverse relationship. Finally, the bottom-right plot illustrates a weak positive correlation between PET and wind speed (V_s), with the equation $y=3.6376x+30.924$ and a low ($R^2 = 0.0616$), reflecting a weak and poorly fitting relationship. Overall, PET is shown to have the strongest correlations with (T_{mrt}) then with (T_a) and (H_r) but only a weak association with wind speed.

3.6 Universal Thermal Climate Index (UTCI) variations

The same observations were made with regard to the PET, it is clear in (Fig. 11) that the (T_{mrt}) has a direct influence on the curves of the three stations and this mainly due to the solar masks offered by the canopy of trees and the refreshing effect that the latter offer.

The measurements at Station S2 showed notably more comfortable conditions compared to S1(600dwl) and S3(downtown). The average UTCI readings were 31.5°C, 33.9°C, and 34.7°C for S2, S3, and S1 respectively, indicating that S1 experiences the most uncomfortable conditions among the three locations.

The highest UTCI readings were recorded at 14:00, with S2 at 40.3°C, S3 at 43.1°C, and S1 at 46.4°C. The lowest values, observed at 06:00, were 23.9°C for S2, 24.6°C for S3, and 25.2°C for S1. In contrast to the PET findings (fig. 8) where S1 showed better comfort during nighttime, a comparison between S1 (600dwl) and S3 (downtown) revealed that S3 generally provided more comfortable thermal conditions than S1 throughout the day. This difference was most pronounced at midday, with the largest gap (3.3°C) occurring at 14:00, except at 03:00 and 18:00. Similar to the PET analysis, the UTCI curve for S3 showed a depression between 13:00 and 16:00, primarily due to the solar mask effect in the canyon.

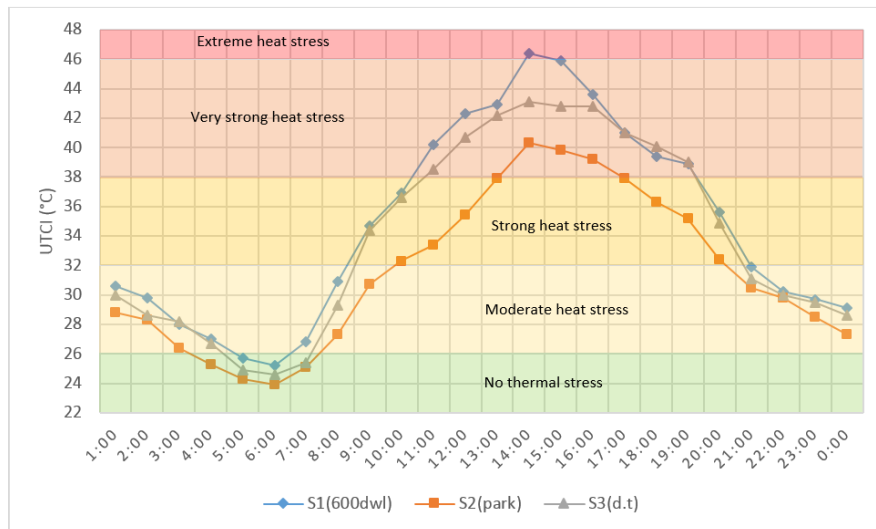


Fig 11. Universal Thermal Climate Index (UTCI) for three sites of investigation.

In terms of comfort zones, the data showed varying durations of thermal comfort for different stations. Station S2 experienced no thermal stress for approximately 4 hours and 15 minutes (from 3:15 to 7:30), accounting for 17.7% of the day. Station S3 recorded 2 hours and 45 minutes (from 4:30 to 7:15) within

the comfort zone, which was 11.45% of the total time. Finally, station S1 had the shortest period of thermal comfort, averaging only 1 hour and 35 minutes (from 4:55 to 6:30), or 6.6% of the entire day.

In the Very Strong heat stress zone, the curve of station S2 fell within this range for only 4 hours (13:00-17:00), accounting for 16.6% of the total duration. In contrast, S3 spent 8:30 hours (35.4%), while S1 remained there for 9 hours in this zone, equivalent to (37.5%) of the total time. It is worth highlighting that S1 (600dwl) was the only station to enter the Extreme Heat stress zone, lasting approximately 1 hour (4% of total time). This observation confirmed that S1 was the least comfortable among the three stations.

If we group the “No thermal stress zone” and the “moderate heat zone” into a “global comfort zone” we find that station S2(park) is in this area for 13 hours (54.2% of the total time), while S3 records 10:45 (44.8% of the total time) and S1 10:15 (42.7% of the total time). On the other hand, if we group the discomfort zones (Strong heat stress-Very strong heat stress-Extreme heat stress) into a global discomfort zone, station S2 records 11 hours in this zone (45.8% of the total time) and S3 records 13:15 (55.2% of the total time) and S1 13:45 (57.3% of the total time). confirming even more that the S2 station (park) is far more comfortable and that it benefits greatly from the effect of the cool island created by the communal park.

Figure (12) illustrate the relationships between the Universal Thermal Climate Index (UTCI) and various environmental parameters. The UTCI versus Tmrt (Mean Radiant Temperature) graph shows a strong positive correlation ($R^2 = 0.913$), with UTCI increasing as radiant temperature rises. The UTCI versus Ta (Air Temperature) plot demonstrates an even stronger positive correlation ($R^2 = 0.9676$), indicating that UTCI increases more steeply with air temperature compared to radiant temperature. Conversely, the UTCI versus Hr (Relative Humidity) graph reveals a strong negative correlation ($R^2 = 0.8931$), where UTCI decreases as relative humidity increases.

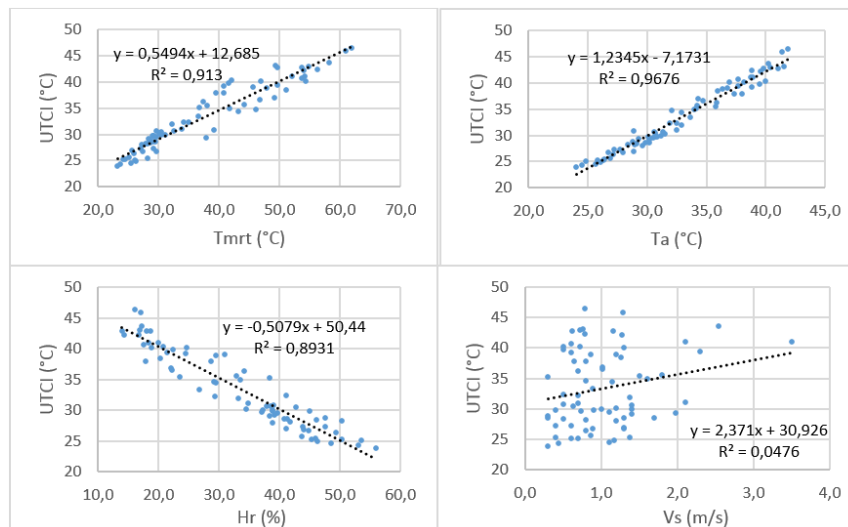


Fig 12. Correlation between (UTCI) and various environmental parameters.

The UTCI versus Wind Speed plot shows a very weak positive correlation ($R^2 = 0.0476$) with a large scatter of points, suggesting little clear relationship between wind speed and UTCI. Overall, these graphs indicate that air temperature has the strongest influence on UTCI, followed closely by mean radiant temperature, while relative humidity has a significant inverse effect. Wind speed appears to have minimal impact on UTCI in this dataset. The UTCI values range from about 20 to 50, suggesting a wide range of thermal comfort conditions. These relationships between UTCI and environmental factors

appear similar to those observed with PET in (Fig. 9), reflecting UTCI's design to be applicable across various climates, seasons, and scales.

3.7 Predicted Mean Vote (PMV) variations

As with the PET, the S2 station records significantly lower and therefore more comfortable values than those of S1(600dwl) and S3(downtown). With an average PMV value of 1.06 for S2, 2.34 for S3 and 2.56 for S1, making the latter the most uncomfortable of the three stations.

Maximum PMV values were 3.74 at 14:00 for S2, 5.36 at 16:00 for S3 and 6.83 at 14:00 for S1. Minimum values (all recorded at 06:00) are -1.23 for S2, -1.04 for S3 and -0.88 for S1. When comparing S1 (600dwl) and S3 (downtown), we noticed that S3 was generally more comfortable than S1 between 6:00 and 19:00 (equivalent to sunrise and sunset), especially in the middle of the day when the gap between the two stations was maximal. The crushing (pulling down) of the S3 curve (between 13:00 and 16:00) was mainly due to the physical solar mask (buildings) south of the canyon.

This trend is reversed before 6:00 (before sunrise) and after 15:00 (after sunset), when the PMV curve of station S1 is lower than that of S3 and, therefore, relatively more comfortable. This is explained by the fact that station S1 is located in an open space with a large opening to the sky, which allows heat gains captured during the day to escape, unlike station S3, which has a smaller opening to the sky, in addition to the releasing of the heat gains captured during the day by the canyon walls.

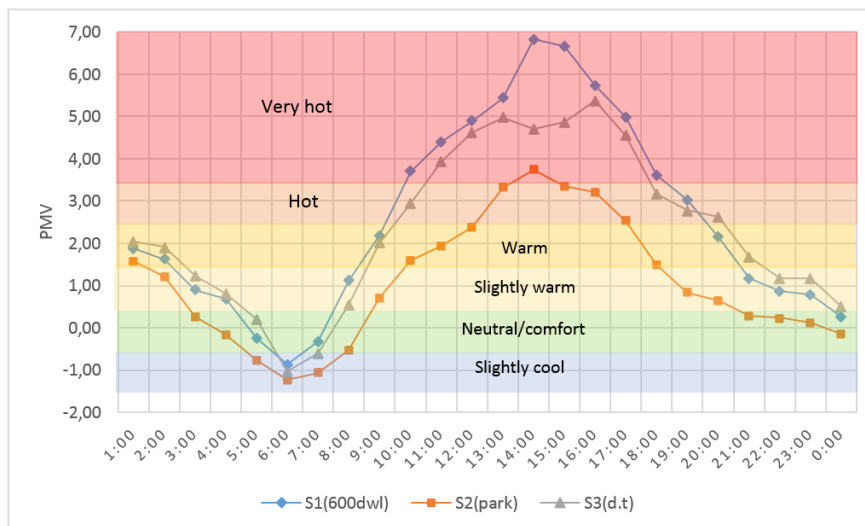


Fig 13. Predicted Mean Vote (PMV) for three sites of investigation.

Regarding the comfort zones, we notice that the curve of station S2 was in the comfortable zones (neutral zone and slightly cool zone) during 9:30 hours (3:00-9:00 and 20:30-00:00), which represents 40% of the total time of the day. On the other hand, the curves of stations S1 and S3 were in this zone for only 4 hours on average (4:00-8:00), which represents 16% of the total time.

For the discomfort zone (hot and very hot), the curve of station S2 was situated in this zone for 5 hours (12:00-17:00), representing 20% of the total time, and 10:30 hours for stations S1 and S3 on average, representing 43% of the total time.

It should be noted that the PMV curve of S2 touched the maximum discomfort zone (very hot zone), equivalent to a PMV greater than 3.5 for less than 1 hour around 14:00, representing 4% of the total time, whereas S1 and S3 recorded approximately 8 hours in this zone (between 10:00 and 18:00) or 33% of the total time of the day.

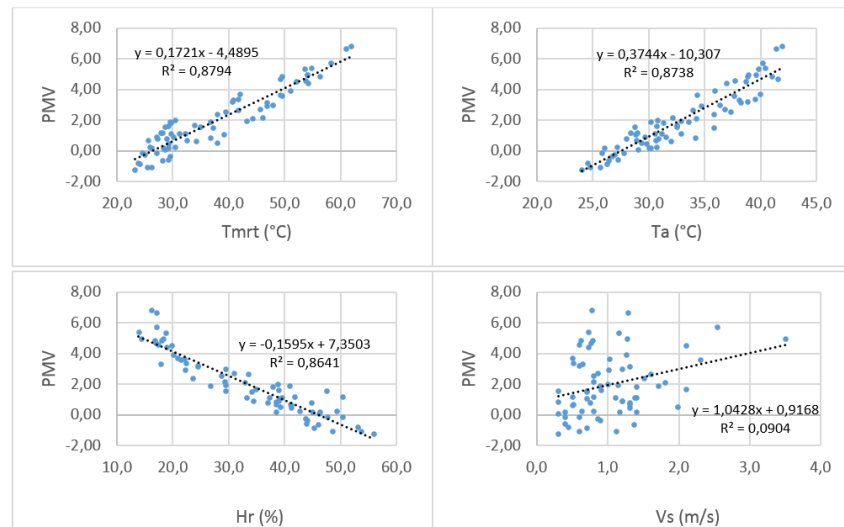


Fig 14. Correlation between (PMV) and various environmental parameters.

Figure (14) shows four scatter plots illustrating the relationship between the Predicted Mean Vote (PMV) and various environmental parameters. The graph of PMV versus Tmrt (Mean Radiant Temperature) shows a strong positive correlation ($R^2 = 0.8794$), with PMV increasing as Tmrt increased. Similarly, the PMV versus Ta (Air Temperature) graph demonstrates a strong positive correlation ($R^2 = 0.8738$), indicating that PMV increases with air temperature. In contrast, the PMV versus Hr (Relative Humidity) plot reveals a strong negative correlation ($R^2 = 0.8641$), where PMV decreases as relative humidity increases. The PMV versus Vs (Wind Speed) graph shows a weak positive correlation ($R^2 = 0.0904$) with a less clear relationship and a large scatter of points. Overall, these graphs suggest that both radiant and air temperatures have the strongest impact on PMV, while relative humidity has a significant inverse effect. The wind speed appears to have less influence on the PMV in this dataset. Notably, the PMV values range from about -2 to 8, exceeding the standard scale of -3 to +3, which suggests the presence of extreme thermal conditions. These visualizations provide valuable insights into how different environmental factors influence thermal comfort as measured by PMV.

These relationships between PMV and the four environmental factors appear also similar to those observed with PET (Fig. 10) and UTCI (Fig. 12), but with different scaling and sensitivity.

3.8 Predicted Percentage of Dissatisfied (PPD) variations

According to the Predicted Percentage of Dissatisfied (PPD) depicted in Fig. 15, the average level of dissatisfaction at station S2 (park) was 43.2%, which was lower than that of S1 (61.6%) and S3 (65.6%). The maximum difference between S1 and S2 was 68.6% at 19h00, whereas the difference between S3 and S2 was 61.7% at 20h00. Indeed, if we return to the PMV values at this interval (19:00-20:00) we note that S2 reaches the comfort zone equivalent to values below 0.5 while S1 and S3 are still in the discomfort zone (Warm) with values above 2.5.

For S1 and S3, the dissatisfaction rate reached 100% from 10:00 to 19:00 (for 9 hours), while for S2, this was reached from 13:00 to 16:00 (for only 3 hours).

It is important to point out that during the period 5:00-7:00, the dissatisfaction rate was higher at the park (S2) than at the two other sites, due to negative PMV values during this time (slightly cool period) resulting from the morning freshness, and not due to heat.

Our results highlight the importance of urban parks as significant contributors to the thermal comfort in urban areas. By analyzing the data collected, we observed a significant reduction in weather parameters

such as air temperature (T_a) and mean radiant temperature (T_{mrt}) as well as comfort indices combining these different weather variables to better represent the actual thermal sensation experienced by the individual such as PET, PMV and UTCI in the surrounding areas, especially during periods of extreme heat. This decrease in temperature is attributed to the natural cooling effect of green spaces, which promotes heat dissipation and local thermal regulation.

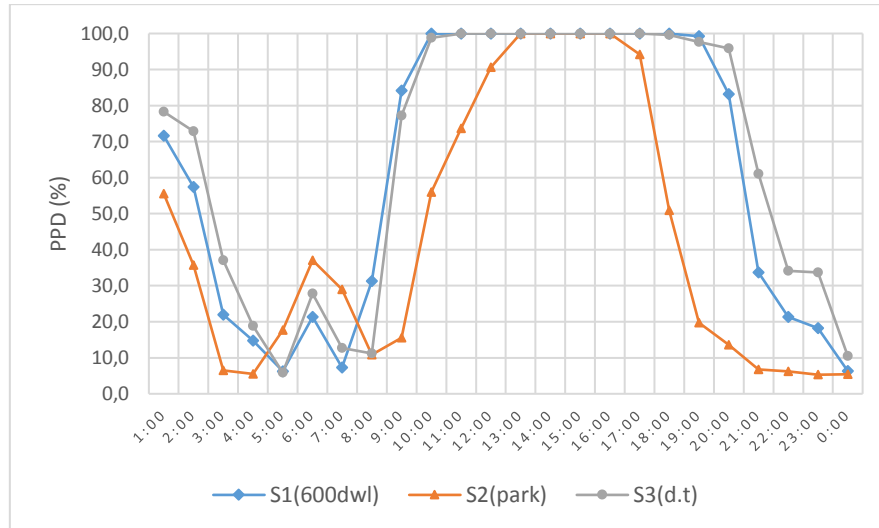


Fig 15. Predicted Percentage of Dissatisfied (PPD) for three sites of investigation.

These observations are consistent with those of previous work in several studies, such as those of Bilgili et al. (2013), Heusinkveld et al. (2014), Yan et al. (2018) and Amani-Beni et al. (2021) which highlighted the importance of urban parks in reducing urban heat island (UHI) and improving the thermal comfort of residents. Our research confirms the importance of integrating these elements into urban planning strategies to ensure sustainable and resilient urban environments for climate change challenges.

While the results obtained from our measurements may appear conventional at first glance, their originality lies in the fact that this is the first study of its kind conducted in the city of Sétif and in such a specific context. This study establishes a reference point for understanding the microclimatic effects of urban parks in semi-arid climates, providing a valuable baseline for future research. Furthermore, these findings contribute significantly to the existing literature on urban heat mitigation and outdoor thermal comfort, enriching the scientific understanding of these phenomena in understudied regions.

Several aspects of originality in our results stand out:

- **High UHI Intensity:** The study identifies a maximum urban heat island (UHI) intensity of 4.4°C , which is higher than values reported in many other studies. This highlights the severity of the UHI effect in Sétif and underscores the need for targeted mitigation strategies.
- **Significant Cooling Effect:** The urban park demonstrated a cooling effect of -3.3°C compared to surrounding urban areas. This finding suggests that vegetation plays an even more critical role in arid and semi-arid environments, where impervious surfaces tend to amplify heat retention.
- **Quantified Parameter Impact:** Based on our measurements, we were able to quantify the influence of each parameter on the studied thermal comfort indices. This analysis confirmed the dominant role of air temperature and mean radiant temperature (T_{mrt}) in shaping thermal comfort.

- **Limited Wind Impact:** Unlike studies conducted in temperate climates, which often show a strong correlation between wind and thermal comfort, our results suggest that wind has a minor effect in semi-arid climates. This could be a local specificity and warrants further investigation to better understand its implications.

These results constitute an empirical database for the region, particularly for Sétif, offering essential insights to guide future urban planning policies and strategies aimed at reducing urban heat islands in similar climatic contexts. By providing detailed, contextual and specific data, our study not only advances scientific knowledge but also supports practical decision-making for sustainable urban development in semi-arid regions.

We acknowledge that a comprehensive diagnostic analysis incorporating all potential contributing factors to the Urban Heat Island (UHI) effect would have provided a more complete understanding of the thermal dynamics observed in this study. While our research demonstrates significant temperature differences between the urban park and surrounding urban areas, a complete attribution of these differences would require detailed analysis of multiple additional parameters including surface material properties, thermal inertia, anthropogenic heat from human activities, urban pollution levels, and three-dimensional urban geometry. Such an exhaustive multi-parameter analysis was beyond the scope of the current study due to equipment limitations, resource constraints, and the specific focus of our research objectives.

Our methodology prioritized reliable, direct measurements of key meteorological parameters (air temperature, relative humidity, wind speed, and mean radiant temperature) to quantify the cooling effect of the urban park compared to urban sites. While this approach provides robust empirical evidence of the park's cooling capacity, we cannot definitively isolate the exact contribution of vegetation from other mitigating factors without further controlled studies. This limitation should be considered when interpreting our findings regarding the dominant role of green spaces in UHI mitigation.

We propose that future research in this geographical context should build upon our findings by incorporating more comprehensive parameter measurements, including surface albedo analysis, anthropogenic heat flux quantification, and three-dimensional urban canyon assessments, to develop a more complete diagnostic framework for UHI formation and mitigation strategies in semi-arid North African cities. Such extended analyses would further strengthen the scientific understanding of urban microclimate dynamics in understudied geographical regions.

4. CONCLUSION

This study aimed to examine the benefits of Sétif City's urban park (semi-arid climate) on outdoor thermal comfort by comparing it with its surroundings, specifically the 600 dwellings neighborhood to the north and the old city center to the south, two densely urbanized fabrics with different typologies and configurations.

The results first confirmed the presence of the urban heat island (UHI) phenomenon in Sétif City, with a maximum difference of 4.4°C between the city center and the peripheral weather station. Only the park recorded values lower than the periphery, with a difference reaching up to 1.3°C.

Comparative analysis revealed significantly more favorable thermal conditions in the park at all levels. Air temperature showed an average difference of 2.1°C between the park and urbanized sites, with a maximum of 3.3°C. Relative humidity was significantly higher in the park, with an average difference of 8.6% and a maximum difference of 12.7%. The Mean Radiant Temperature (T_{mrt}) in the park displayed a daily average of 32.5°C compared to 41.1°C for the most exposed urban area.

Thermal comfort indices confirmed this trend. The average Physiological Equivalent Temperature (PET) was 31.7°C in the park versus 36.8°C in the 600 dwellings area. The Predicted Mean Vote (PMV) also confirmed better comfort in the park with an average of 1.06 compared to 2.56 for urban areas. The Predicted Percentage of Dissatisfied (PPD) was lowest in the park at 43.2%, compared to over 60% in urbanized areas.

Correlation analysis between the three thermal comfort indices (PET, UTCI, and PMV) and environmental parameters revealed consistent patterns. The mean radiant temperature (T_{mrt}) and air temperature (T_a) showed the strongest positive correlations ($R^2 > 0.87$), whereas relative humidity exhibited a strong negative correlation ($R^2 > 0.86$). Wind velocity demonstrated a minimal influence on the three indices.

These findings highlight the importance of urban vegetation, particularly tree canopies, in regulating the urban microclimate through shading and evapotranspiration. The Sétif Park thus offers significantly superior comfort conditions compared to adjacent neighborhoods, encouraging architectural and urban design stakeholders to integrate nature into their projects, especially in arid and semi-arid climates.

While this study has produced concrete and conclusive results, future research could expand upon these findings using geographic information systems (GIS) and remote sensing to analyze the thermal comfort distribution on a broader scale.

NOMENCLATURE

Hr	Relative Humidity [%]	T_a	Air temperature [°C]
PET	Physiologically equivalent temperature	T_{mrt}	Mean radiant temperature
PMV	Predicted Mean Vote	UTCI	Universal Thermal Climate Index
PPD	Predicted Percentage of Dissatisfied	V	Wind Speed [m/s]

REFERENCES

- Abd Elraouf, R., Elmokadem, A., Megahed, N., Abo Eleinen, O., & Eltarabily, S. (2022). The impact of urban geometry on outdoor thermal comfort in a hot-humid climate. *Building and Environment*, 225. <https://doi.org/10.1016/j.buildenv.2022.109632>.
- Akbari, H., & Akbari, H. (2005). *Passive and Low Energy Cooling 11 for the Built Environment*. <https://www.researchgate.net/publication/254744057>.
- Algretawee, H. (2022). The effect of graduated urban park size on park cooling island and distance relative to land surface temperature (LST). *Urban Climate*, 45. <https://doi.org/10.1016/j.uclim.2022.101255>.
- Alonzo, M., Baker, M. E., Gao, Y., & Shandas, V. (2021). Spatial configuration and time of day impact the magnitude of urban tree canopy cooling. *Environmental Research Letters*, 16(8). <https://doi.org/10.1088/1748-9326/ac12f2>.
- Alves, F. M., Gonçalves, A., & Enjuto, M. R. D. C. (2022). The Use of Envi-Met for the Assessment of Nature-Based Solutions' Potential Benefits in Industrial Parks—A Case Study of Argales Industrial Park (Valladolid, Spain). *Infrastructures*, 7(6). <https://doi.org/10.3390/infrastructures7060085>.

- Amani-Beni, M., Zhang, B., Xie, G. Di, & Odgaard, A. J. (2021). Impacts of the microclimate of a large urban park on its surrounding built environment in the summertime. *Remote Sensing*, 13(22). <https://doi.org/10.3390/rs13224703>.
- Ballout, A., Bouchahm, Y., & Lacheheb, D. E. Z. (2016). Urban quality through Thermal Comfort Conditions in an Urban Space. The Square of Independence, Sétif, Algeria. 12th International Symposium on Urban Planning and Environment, 148–161. <https://doi.org/10.1016/j.amepre.2009.09.012>.
- Ballout, A., Lacheheb, D. E. Z., & Bouchahm, Y. (2015). Improvement of Thermal Comfort Conditions in an Urban Space (Case Study: The Square of Independence, Sétif, Algeria). *European Journal of Sustainable Development*, 4(2). <https://doi.org/10.14207/ejsd.2015.v4n2p407>.
- Bilgili, B. C., Şahin, Ş., Yilmaz, O., Gürbüz, F., & Arici, Y. K. (2013). Temperature distribution and the cooling effects on three urban parks in Ankara, Turkey. *International Journal of Global Warming*, 5(3), 296–310. <https://doi.org/10.1504/IJGW.2013.055364>.
- Błażejczyk, K., Jendritzky, G., Bröde, P., Fiala, D., Havenith, G., Epstein, Y., Psikuta, A., & Kampmann, B. (2013). An introduction to the Universal thermal climate index (UTCI). *Geographia Polonica*, 86(1), 5–10. <https://doi.org/10.7163/GPol.2013.1>.
- Bouketta, S., & Bouchahm, Y. (2023). L'effet de la géométrie urbaine sur l'écoulement du vent et la ventilation naturelle extérieure. *Journal of Renewable Energies*, 15(4). <https://doi.org/10.54966/jreen.v15i4.353>.
- Boukhelkhal, I., & Bourbia, P. F. (2016). Thermal Comfort Conditions in Outdoor Urban Spaces: Hot Dry Climate -Ghardaia- Algeria. *Procedia Engineering*, 169, 207–215. <https://doi.org/10.1016/j.proeng.2016.10.025>.
- Bowler, D. E., Buyung-Ali, L., Knight, T. M., & Pullin, A. S. (2010). Urban greening to cool towns and cities: A systematic review of the empirical evidence. *Landscape and Urban Planning*. 97(3), 147–155. <https://doi.org/10.1016/j.landurbplan.2010.05.006>.
- Bröde, P. (2021). Issues in UTCI Calculation from a Decade's Experience. In *Applications of the Universal Thermal Climate Index UTCI in Biometeorology* (pp. 13–21). Springer International Publishing. https://doi.org/10.1007/978-3-030-76716-7_2.
- Bröde, P., Fiala, D., Błażejczyk, K., Holmér, I., Jendritzky, G., Kampmann, B., Tinz, B., & Havenith, G. (2012). Deriving the operational procedure for the Universal Thermal Climate Index (UTCI). *International Journal of Biometeorology*, 56(3), 481–494. <https://doi.org/10.1007/s00484-011-0454-1>.
- Busato, F., Lazzarin, R. M., & Noro, M. (2014). Three years of study of the Urban Heat Island in Padua: Experimental results. *Sustainable Cities and Society*, 10, 251–258. <https://doi.org/10.1016/j.scs.2013.05.001>.
- Carne, R. J., 1994. Urban vegetation: ecological and social value. In: *A Vision for a Greener City. The Role of Vegetation in Urban Environment. Proceedings: 1994 National Greening Australia Conference* (October 4, 5 & 6, Fremantle, WA), Ed. M.A. Scheltema (Greening Australia Ltd, Canberra): 211-225.
- Chang, C. R., & Li, M. H. (2014). Effects of urban parks on the local urban thermal environment. *Urban Forestry and Urban Greening*, 13(4), 672–681. <https://doi.org/10.1016/j.ufug.2014.08.001>.
- Chen, Y. C. (2023). Thermal indices for human biometeorology based on Python. *Scientific Reports*, 13(1), 20825. <https://doi.org/10.1038/s41598-023-47388-y>.

- Chen, Y., & Wong, N. H. (2006). Thermal benefits of city parks. *Energy and Buildings*, 38(2), 105–120. <https://doi.org/10.1016/j.enbuild.2005.04.003>.
- Choi, H. A., Lee, W. K., & Byun, W. H. (2012). Determining the effect of green spaces on Urban heat distribution using satellite imagery. *Asian Journal of Atmospheric Environment*, 6(2), 127–135. <https://doi.org/10.5572/ajae.2012.6.2.127>.
- Corocăescu, A., Ichim, P., Crețu, C. Ștefănel, & Sfică, L. (2023). Assessment of Climate Characteristics of an Urban Park Using Satellite Imagery and In-Situ Measurements. Study Case of Cancicov Park from Bacău City (Romania). *Babes Bolyai University Faculty of Geography*. ISSN2067743X). 33–46. <https://doi.org/10.24193/AWC202304>.
- Dec, E., Babiarez, B., & Sekret, R. (2018). Analysis of temperature, air humidity and wind conditions for the needs of outdoor thermal comfort. *E3S Web of Conferences*, 44. <https://doi.org/10.1051/e3sconf/20184400028>.
- Du, Y., & Mak, C. M. (2018). Improving pedestrian level low wind velocity environment in high-density cities: A general framework and case study. *Sustainable Cities and Society*, 42, 314–324. <https://doi.org/10.1016/j.scs.2018.08.001>.
- Edwards, P. J., Drillet, Z., Richards, D. R., Fung, T. K., & Song, X. P. (2020). Benefits of tropical urban vegetation. Singapore-ETH Centre, Future Cities Laboratory. <https://fcl.ethz.ch/news-events/news/2020/07/benefits-of-tropical-urban-vegetation.html>.
- Fang, Z., Feng, X., & Lin, Z. (2017). Investigation of PMV Model for Evaluation of the Outdoor Thermal Comfort. *Procedia Engineering*, 205, 2457–2462. <https://doi.org/10.1016/j.proeng.2017.09.973>.
- Gatto, E., Buccolieri, R., Aarrevaara, E., Ippolito, F., Emmanuel, R., Perronace, L., & Santiago, J. L. (2020). Impact of Urban vegetation on outdoor thermal comfort: Comparison between a Mediterranean city (Lecce, Italy) and a northern European city (Lahti, Finland). *Forests*, 11(2). <https://doi.org/10.3390/f11020228>.
- Hanafi, A., & Alkama, D. (2016). Stratégie d’amélioration du confort thermique d’une place publique d’une ville saharienne “Biskra/Algérie.” *Journal of Renewable Energies*, 19(3), 465–480. <https://doi.org/10.54966/jreen.v19i3.585>.
- Heusinkveld, B. G., Steeneveld, G. J., Van Hove, L. W. A., Jacobs, C. M. J., & Holtslag, A. A. M. (2014). Spatial variability of the rotterdam urban heat island as influenced by urban land use. *Journal of Geophysical Research*, 119(2), 677–692. <https://doi.org/10.1002/2012JD019399>.
- Holst, J., & Shashua-Bar, L. (2010). Comparative study of trees impact on human thermal comfort in urban streets under hot-arid and temperate climates. <https://www.researchgate.net/publication/303189153>.
- Höppe P. (1999). The physiological equivalent temperature – a universal index for the biometeorological assessment of the thermal environment. *Int J Biometeorol* 43, 71–75. <https://doi.org/10.1007/s004840050118>.
- Huang, Z., Wu, C., Teng, M., & Lin, Y. (2020). Impacts of tree canopy cover on microclimate and human thermal comfort in a shallow street canyon in Wuhan, China. *Atmosphere*, 11(6). <https://doi.org/10.3390/atmos11060588>.
- Huerta, R. E., Yépez, F. D., Lozano-García, D. F., Cobián, V. H. G., Fierro, A. L. F., Gómez, H. de L., González, R. A. C., & Vargas-Martínez, A. (2021). Mapping urban green spaces at the metropolitan

- level using very high resolution satellite imagery and deep learning techniques for semantic segmentation. *Remote Sensing*, 13(11). <https://doi.org/10.3390/rs13112031>.
- Huryna, H., & Pokorný, J. (2016). The role of water and vegetation in the distribution of solar energy and local climate: a review. *Folia Geobotanica*, 51(3), 191–208. <https://doi.org/10.1007/s12224-016-9261-0>.
- Jauregui, E. (1990). Influence of a Large Urban Park on Temperature and Convective Precipitation in a Tropical City. *Energy and Buildings*, 15(3–4), 457–463, [https://doi.org/10.1016/0378-7788\(90\)90021-A](https://doi.org/10.1016/0378-7788(90)90021-A).
- Konijnendijk, C.C., Annerstedt, M., Nielsen, A. B., Maruthaveeran, S., (2013). Benefits of Urban Parks: A systematic review. A Report for IFPRA. <https://parksleisure.com.au/wp-content/uploads/parc-library/113-0-IfpraBenefitsOfUrbanParks.pdf>.
- Kulish, T. (2022). Spatial variation of soil temperature fields in an urban park. *IOP Conference Series: Earth and Environmental Science*, 1049(1). <https://doi.org/10.1088/1755-1315/1049/1/012056>.
- Laouadi, A. (2022). A New General Formulation for the PMV Thermal Comfort Index. *Buildings*, 12(10). <https://doi.org/10.3390/buildings12101572>.
- Lenzuni, P. (2021). Compliance with limits of acceptability for thermal comfort, and implications for long-term comfort. *Building and Environment*, 204. <https://doi.org/10.1016/j.buildenv.2021.108067>.
- Li, L., Zhou, X., & Yang, L. (2017). The Analysis of Outdoor Thermal Comfort in Guangzhou during Summer. *Procedia Engineering*, 205, 1996–2002. <https://doi.org/10.1016/j.proeng.2017.10.070>.
- Liu, Z., Li, J., & Xi, T. (2023). A Review of Thermal Comfort Evaluation and Improvement in Urban Outdoor Spaces. In *Buildings*, 13(12). Multidisciplinary Digital Publishing Institute (MDPI). <https://doi.org/10.3390/buildings13123050>.
- Matallah, M. E., Alkama, D., Ahriz, A., & Attia, S. (2020). Assessment of the outdoor thermal comfort in oases settlements. *Atmosphere*, 11(2). <https://doi.org/10.3390/atmos11020185>.
- Matzarakis, A., Muthers, S., & Rutz, F. (2014). Application and comparison of UTCI and pet in temperate climate conditions. *Finisterra*, 49(98), 21–31. <https://doi.org/10.18055/Finis6453>.
- Mayer, H., Kuppe, S., Holst, J., Imbery, F., & Matzarakis, A. (2009). Human thermal comfort below the canopy of street trees on a typical Central European summer day. <https://www.researchgate.net/publication/22850675>.
- McIntyre, D. (1973). A guide to thermal comfort. *Applied Ergonomics*, 4(2), 66–72. [https://doi.org/10.1016/0003-6870\(73\)90079-3](https://doi.org/10.1016/0003-6870(73)90079-3).
- Memon, A.R., Leung, D. Y., & Chunho, L. (2008). A review on the generation, determination and mitigation of Urban Heat Island. *Journal of Environmental Sciences* 20. 120–128.
- Mikami, T., Sugawara, H., Shimizu, S., Hagiwara, S., & Narita, K.-I. (2015). How much does urban green cool town? <https://www.researchgate.net/publication/280534513>.
- Mills, G. (2008). Luke Howard and The Climate of London. *Weather*, 63(6), 153–157. <https://doi.org/10.1002/wea.195>.
- Nicol, F. (2004). Adaptive thermal comfort standards in the hot-humid tropics. *Energy and Buildings*, 36(7), 628–637. <https://doi.org/10.1016/j.enbuild.2004.01.016>.
- Nicol, J. F., & Humphreys, M. A. (2002). Adaptive thermal comfort and sustainable thermal standards for buildings. *Energy and Buildings*, 34(6), 563–572. [https://doi.org/10.1016/S0378-7788\(02\)00006-3](https://doi.org/10.1016/S0378-7788(02)00006-3).

- Nuruzzaman, Md. (2015). Urban Heat Island: Causes, Effects and Mitigation Measures - A Review. *International Journal of Environmental Monitoring and Analysis*, 3(2), 67. <https://doi.org/10.11648/j.ijema.20150302.15>.
- Oke T.R. (1987). *Boundary Layer Climates*. Taylor & Francis. <https://doi.org/10.4324/9780203407219>.
- Paris, M., Sansen, M., Bosc, S., & Devillers, P. (2022). Simulation Tools for the Architectural Design of Middle-Density Housing Estates. *Sustainability*, 14(17). <https://doi.org/10.3390/su141710696>.
- Park, J., Kim, J. H., Sohn, W., & Lee, D. K. (2021). Urban cooling factors: Do small greenspaces outperform building shade in mitigating urban heat island intensity? *Urban Forestry and Urban Greening*, 64. <https://doi.org/10.1016/j.ufug.2021.127256>.
- Pezzoli, A., Cristofori, E., Gozzini, B., Marchisio, M., & Padoan, J. (2012). Analysis of the thermal comfort in cycling athletes. *Procedia Engineering*, 34, 433–438. <https://doi.org/10.1016/j.proeng.2012.04.074>.
- Qin, H., Cheng, X., Han, G., Wang, Y., Deng, J., & Yang, Y. (2021). How thermal conditions affect the spatial-temporal distribution of visitors in urban parks: A case study in Chongqing, China. *Urban Forestry and Urban Greening*, 66. <https://doi.org/10.1016/j.ufug.2021.127393>.
- Qiu, X., Kil, S. H., Jo, H. K., Park, C., Song, W., & Choi, Y. E. (2023). Cooling Effect of Urban Blue and Green Spaces: A Case Study of Changsha, China. *International Journal of Environmental Research and Public Health*, 20(3). <https://doi.org/10.3390/ijerph20032613>.
- Ravi, S., & D’Odorico, P. (2005). A field-scale analysis of the dependence of wind erosion threshold velocity on air humidity. *Geophysical Research Letters*, 32(21), 1–4. <https://doi.org/10.1029/2005GL023675>.
- Salameh, M., Elkhazindar, A., & Touqan, B. (2023). The effect of building height on thermal properties and comfort of a housing project in the hot arid climate of the UAE. *Frontiers in Built Environment*, 9. <https://doi.org/10.3389/fbuil.2023.1174147>.
- Santamouris, M. (2007). Heat Island Research in Europe: The State of the Art. *Advances in Building Energy Research*, 1(1), 123–150. <https://doi.org/10.1080/17512549.2007.9687272>.
- Santamouris, M. (2014). Cooling the cities - A review of reflective and green roof mitigation technologies to fight heat island and improve comfort in urban environments. *Solar Energy*, 103, 682–703. <https://doi.org/10.1016/j.solener.2012.07.003>.
- Sanusi, R., Johnstone, D., May, P., & Livesley, S. J. (2016). Street Orientation and Side of the Street Greatly Influence the Microclimatic Benefits Street Trees Can Provide in Summer. *Journal of Environmental Quality*, 45(1), 167–174. <https://doi.org/10.2134/jeq2015.01.0039>.
- Simon, H., Sinsal, T., & Bruse, M. (2021). Advances in simulating radiative transfer in complex environments. *Applied Sciences (Switzerland)*, 11(12). <https://doi.org/10.3390/app11125449>.
- Stark da Silva, P. W., Duarte, D., & Pauleit, S. (2023). The Role of the Design of Public Squares and Vegetation Composition on Human Thermal Comfort in Different Seasons a Quantitative Assessment. *Land*, 12(2). <https://doi.org/10.3390/land12020427>.
- Sugawara, H., Shimizu, S., Takahashi, H., Hagiwara, S., Narita, K., Mikami, T., & Hirano, T. (2016). Thermal Influence of a Large Green Space on a Hot Urban Environment. *Journal of Environmental Quality*, 45(1), 125–133. <https://doi.org/10.2134/jeq2015.01.0049>.
- Sukopp, H., & Werner, P. (1983). Urban environments and vegetation. In *Man’s impact on vegetation* (pp. 247–260). Springer Netherlands. https://doi.org/10.1007/978-94-009-7269-8_19.

- Sunita, Kumar, D., & Shekhar, S. (2021). Spatial distribution analysis of urban blue-green spaces for mitigating excessive heat with earth observation systems. *Environmental Challenges*, 5. <https://doi.org/10.1016/j.envc.2021.100390>.
- Thom, J. K., Coutts, A. M., Broadbent, A. M., & Tapper, N. J. (2016). The influence of increasing tree cover on mean radiant temperature across a mixed development suburb in Adelaide, Australia. *Urban Forestry and Urban Greening*, 20, 233–242. <https://doi.org/10.1016/j.ufug.2016.08.016>.
- van Hoof, J., Schellen, L., Soebarto, V., Wong, J. K. W., & Kazak, J. K. (2017). Ten questions concerning thermal comfort and ageing. *Building and Environment*, 120, 123–133. <https://doi.org/10.1016/j.buildenv.2017.05.008>.
- Walls, W., Parker, N., & Walliss, J. (2015). Designing with thermal comfort indices in outdoor sites. R.H. Crawford and A. Stephan (eds.), *Living and Learning: Research for a Better Built Environment: 49th International Conference of the Architectural Science Association 2015*, 1117–1128. The Architectural Science Association and The University of Melbourne.
- Wong, N. H., & Yu, C. (2005). Study of green areas and urban heat island in a tropical city. *Habitat International*, 29(3), 547–558. <https://doi.org/10.1016/j.habitatint.2004.04.008>.
- Wu, P., Zhang, Y., Fang, Z., & Gao, Y. (2022). Comparison of thermal comfort in different kinds of building spaces: Field study in Guangzhou, China. *Indoor and Built Environment*, 31(1), 186–202. <https://doi.org/10.1177/1420326X20981714>.
- Xiao, X. D., Dong, L., Yan, H., Yang, N., & Xiong, Y. (2018). The influence of the spatial characteristics of urban green space on the urban heat island effect in Suzhou Industrial Park. *Sustainable Cities and Society*, 40, 428–439. <https://doi.org/10.1016/j.scs.2018.04.002>.
- Yan, H., & Dong, L. (2015). The impacts of land cover types on urban outdoor thermal environment: the case of Beijing, China. *Journal of Environmental Health Science and Engineering*, 13(1). <https://doi.org/10.1186/s40201-015-0195-x>.
- Yan, H., Wu, F., & Dong, L. (2018). Influence of a large urban park on the local urban thermal environment. *Science of the Total Environment*, 622–623, 882–891. <https://doi.org/10.1016/j.scitotenv.2017.11.327>.
- Yang, J., Hu, X., Feng, H., & Marvin, S. (2021). Verifying an ENVI-met simulation of the thermal environment of Yanzhong Square Park in Shanghai. *Urban Forestry and Urban Greening*, 66. <https://doi.org/10.1016/j.ufug.2021.127384>.
- Yang, P., Xiao, Z. N., & Ye, M. S. (2016). Cooling effect of urban parks and their relationship with urban heat islands. *Atmospheric and Oceanic Science Letters*, 9(4), 298–305. <https://doi.org/10.1080/16742834.2016.1191316>.
- Zakaria, N. H., Salleh, S. A., Asmat, A., Chan, A., Isa, N. A., Hazali, N. A., & Islam, M. A. (2020). Analysis of Wind Speed, Humidity and Temperature: Variability and Trend in 2017. *IOP Conference Series: Earth and Environmental Science*, 489(1). <https://doi.org/10.1088/1755-1315/489/1/012013>.
- Zhang, K., Yun, G., Song, P., Wang, K., Li, A., Du, C., Jia, X., Feng, Y., Wu, M., Qu, K., Zhu, X., & Ge, S. (2023). Discover the Desirable Landscape Structure of Urban Parks for Mitigating Urban Heat: A High Spatial Resolution Study Using a Forest City, Luoyang, China as a Lens. *International Journal of Environmental Research and Public Health*, 20(4), 3155. <https://doi.org/10.3390/ijerph20043155>.

Websites:

APPA. (2019). Végétation urbaine : les enjeux pour l'environnement et la santé. <https://www.appa.asso.fr/wp-content/uploads/2019/10/Végétation-urbaine-les-enjeux-pour-lenvironnement-et-la-santé.pdf>.

Climat-data. (2023). Climat Sétif. <https://fr.climate-data.org/afrique/algerie/setif/setif-3595/>.

Climate Change Heat Impact & Prevention | Climate CHIP. (2024). <https://climatechip.org/>.

ENVI-met. (2023). BioMet: Calculating the PMV Value. [https://envi-met.info/doku.php?id=apps:biomet_pmv&s\[\]=pmv](https://envi-met.info/doku.php?id=apps:biomet_pmv&s[]=pmv).

Ritchie, H. & Roser, M. (2018) - "Urbanization". Published online at OurWorldInData.org. Retrieved from: '<https://ourworldindata.org/urbanization>'.

United Nations Department of Economic and Social Affairs Population Division. (2018). World Urbanization Prospects The 2018 Revision.